Eur. Phys. J. B **8**, 19–30 (1999)

**THE EUROPEAN PHYSICAL JOURNAL B**

EDP Sciences


# Thermodynamic properties of small amorphous and crystalline Silica particles at low temperatures

A. Nittke[1,2], P. Esquinazi[1,a], H.-C. Semmelhack[1], A.L. Burin[3], and A.Z. Patashinskii[3]

[1] Abt. Supraleitung und Magnetismus, Universität Leipzig, Linnéstrasse 5, 04103 Leipzig, Germany
[2] Physikalisches Institut, Universität Bayreuth, 95440 Bayreuth, Germany
[3] Department of Chemistry and Material Science, Northwestern University, Evanston IL 60208, USA

Received 9 April 1998

**Abstract.** We have measured the low-temperature ($T \leq 1$ K) specific heat and heat release of small amorphous and crystalline $SiO_2$ particles embedded in Teflon and of Vycor. The temperature and time dependence of these properties have been interpreted in terms of the tunneling model. We found that the particle size influences the density of states of tunneling systems of the composite. The smaller the size of the particles the larger is the density of states of tunneling systems $P_0$. Quartz grains with dimensions in the micrometer range show similar glass-like properties as vitreous silica. In comparison with bulk vitreous silica, Vycor shows a much larger $P_0$ in agreement with the behavior we found for small $SiO_2$ particles. We discuss the implication of our results on the origin of the universal low-temperature properties of glasses.

**PACS.** 61.43.Fs Glasses – 65.50.+m Thermodynamic properties and entropy – 63.50.+x Vibrational states in disordered systems

## 1 Introduction

Amorphous materials have common peculiarities at low temperatures. In particular the heat capacity depends linearly on temperature and the thermal conductivity shows a square temperature dependence, quite different from crystalline solids. Anderson, Halperin, Varma and, independently, Phillips [1] introduced phenomenological tunneling systems (TS), *i.e.* low-energy excitations, to explain those anomalies. Despite the great success of this model to explain various low-temperature properties, the nature of these excitations remains unclear as well as their peculiar distribution in energy.

In particular, a large amount of amorphous and disordered materials investigated in the past 30 years indicate a striking universality. From their low-temperature properties one obtains that the ratio

$$C = \frac{P_0 \gamma^2}{\rho v^2} \lessapprox 10^{-3}, \qquad (1)$$

where $P_0$ denotes the density of states of TS, $\gamma$ the coupling constant of TS with phonons, $v$ the sound velocity and $\rho$ the mass density. The inequality in (1) reflects the fact that nearly all amorphous and disordered systems, independently on their composition, show glass-like properties at low temperatures that indicate similar density of states ($P_0$=$1 \ldots 8 \times 10^{38}$ $J^{-1}g^{-1}$ for non-annealed disordered systems) and coupling constant ($\gamma \sim 0.2 \ldots \sim 1$ eV for longitudinal phonons) [2].

The magnitude of the glass-like anomalies depends on $P_0$ and on the coupling $\gamma$, reaching, *but not exceeding* $C \sim 10^{-3}$. In other words, we can find amorphous or disordered systems, that due to their previous thermal history, for example, show weaker glass-like anomalies, *i.e.* a small value of $C$. But it has not yet been possible to find (bulk) systems with $C \gg 10^{-3}$ or with a density of states $P_0$ much larger than for vitreous silica, for example. This is actually the striking *universality* that a microscopic foundation of the tunneling model should clarify.

The aim of this work is to study the thermodynamic properties of small-size systems, *i.e.* systems that due to their small dimensions may provide some hints on the nature of the universality mentioned above. One can conclude using the arguments of the recently published theory of Burin and Kagan (see [3] and also the discussion in [4]) that $P_0$ should be larger for smaller samples if the nature of $P_0$ is related to the elastic interaction between initial two-level systems (TLS) or initial "defects".

The small-size systems used in this work are prepared from powders of micro or nano size grains agglomerated by an external pressure. Since the coupling between different grains is much smaller than that within the same grain the effective size reduces to the size of the single grain. Our experimental data prove that the density of the low energy excitations strongly increases for the low size grains with respect to the bulk sample. As it follows from the heat

[a] e-mail: esquin@physik.uni-leipzig.de

release measurements this effect is related to tunneling excitations and can be interpreted as an increase of their density $P_0$. We note that this effect can be due to the change of the interaction between TLS in low size samples but also due to the effect of the large internal surface of the small grain materials under study.

The paper is organized as follows. In the next section we provide an introduction on the theoretical ideas and results of the interaction theory [3]. In Section 3, details on the experiments and samples characteristics are given. Section 4 is devoted to describe the results and Section 5 we discuss them. The conclusion is given in Section 6.

## 2 Theoretical introduction

Tunneling states in dielectric amorphous solids couple strongly with long wavelength excitations (acoustic phonons). It is assumed that a consequence of this coupling is an interaction between TS according to the law

$$U(R) \sim U_0/R^d. \tag{2}$$

In three dimensions $d = 3$. The importance of dipolar strain interaction between TS was already proposed by Klein *et al.* [5]. Yu and Leggett [6] went beyond the assumption of individual tunneling entities and proposed a scenario for the formation of the universality of the low-temperature properties of glasses based on the picture of defects interacting according to the law $1/R^3$. This scenario was intended to explain the quantitative universality of the thermal conductivity at low temperatures found experimentally by Freeman and Anderson [7], observed also in the acoustic properties of amorphous solids. Actually, the internal friction $Q^{-1}$ and the logarithmic slope of the temperature dependent sound velocity $d\ln(v)/d\ln(T)$ are determined by the product of the TS density $P_0$ and their $1/R^3$ interaction constant $U_0$. The universality of this product leads to the empirical law

$$P_0 \propto \frac{1}{U_0}\cdot \tag{3}$$

Recently, Burin and Kagan [3] showed that the nature of the low-energy excitations is derivable from the model of $1/R^3$ interacting initial defects. They construct a renormalization group approach to investigate the low-energy excitations. The scaling parameter of their theory is the effective size $R$. This size represents the effective radius of the interaction. The long-range character of the interaction provides the logarithmic dependence of the density of states $P_0$ on the maximum radius or system size $L$

$$P(\Delta, \Delta_0) = P_0/\Delta_0, \tag{4}$$

with

$$P_0 \approx \frac{10^{-2}}{U_0 \ln(L/a)}\cdot \tag{5}$$

The parameters $\Delta$ and $\Delta_0$ stand for the asymmetry of the double-well potential and tunneling amplitude of TS respectively, and $a$ is the characteristic minimum distance which can be of the order of the interatomic one. Equation (4) has been introduced *phenomenologically* in [1] as a basic assumption of the tunneling model to explain the anomalous properties of amorphous solids. Within the renormalization group analysis developed in [3], this dependence of the density of states on the tunneling amplitude (and its independence on the asymmetry, see Eq. (4)) has been obtained with the density of states $P_0$ defined in equation (5). It has been argued that equation (5) describes the universality of the anomalous glassy properties both quantitatively and qualitatively, because it explains the universality of the product $P_0U_0 \sim 10^{-3}$ observed in glasses, with $U_0 \simeq \gamma^2/\rho v^2$.

It is important that this distribution of the low-energy excitations is only *weakly* sensitive to the properties of the system without interaction; only the parameter $a$ enters in the expression for $P_0$. This is compatible with the experimental observation that very different glasses show similar properties. However, this universality appears for some minimum size of a system $L_* > a$. For smaller size the density of states can strongly differ from that predicted by equation (5) as well as the dependence of the distribution function of the excitations on the tunneling amplitude can be different from the one given by equation (4).

The maximum radius $R_{max}$ for the interaction between TS can be defined by the sample size $L$ at low enough temperatures, or by the temperature dependent correlation radius

$$R_T \propto (U_0/T)^{1/3}. \tag{6}$$

For a bulk sample $R_T \sim 10$ nm at $T \sim 1$ K. Note that the presence of an enhanced internal surface can increase this estimate.

If the distance between defects is larger than the thermal correlation radius $R_T$, then the interaction energy is smaller than the thermal energy and no significant influence on the thermal properties of the system should be observed. If the temperature is low enough ($T < \frac{U_0}{L^3}$) then the maximum radius $R_{max}$ is equal to the size of the sample $L$. Consequently, the properties of the system may become sensitive to the size of the sample.

To be precise, the theoretical results mentioned above are related to the radius of the interaction and *not to the system geometrical size*. The effect of the internal surface may be remarkable. The surface can have its own type of two-level excitations like itinerant dangling bonds which can be much more mobile under the conditions of a free-volume like surrounding than within the bulk. This restricts the direct use of the theory of reference [3].

The materials used in this work have unusual properties not completely covered by any existing theory. The experimental results shown in this work will stimulate further theoretical work to explain the behavior of this class of systems.

**Table 1.** Samples names and characteristics. $\alpha = m_{SiO_2}/m_{total}$ is the mass fraction of $SiO_2$ in the mixture. All powder samples were compacted with a pressure of 1200 bar, with expection of sample S5, which pressure was 40 bar (LP: low pressure).

| Samples | Particle size $SiO_2$ ($\mu$m) | $m$ (g) $SiO_2$ | $\alpha$ | $m_{Tef}$ (g) (powder) | $m_{Tef}$ (g) (total) | $m_{total}$ (g) | Remarks |
|---|---|---|---|---|---|---|---|
| S1 | 0.02 | 9.9 | 50% | 9.9 | 20.9 | 30.8 | Vitreous Silica + Teflon |
| S2 | 0.004 | 9.3 | 50% | 9.3 | 19.5 | 28.8 | Vitreous Silica + Teflon |
| S3 | 0.02 | 2.0 | 14% | 11.9 | 19.4 | 21.4 | Vitreous Silica + Teflon |
| S4 | 20 | 13.9 | 50% | 13.9 | 24.7 | 38.6 | Quartz + Teflon |
| S5 | 20 | 8.7 | 50% | 8.7 | 20.0 | 28.7 | Quartz + Teflon (LP) |
| S6 | 5 | 10.2 | 50% | 10.2 | 20.7 | 30.9 | Quartz + Teflon |
| S7 | 1 | 13.1 | 50% | 13.1 | 23.7 | 36.9 | Quartz + Teflon |
| S8 | 1 | 14.0 | 75% | 4.6 | 14.4 | 28.6 | Quartz + Teflon |
| S9 | – | – | – | 20.9 | 28.1 | 28.1 | Teflon |
| V1 | – | 19.0 | 70% | – | 8.3 | 27.3 | Vycor (Pore radius $\sim$ 3 nm) |

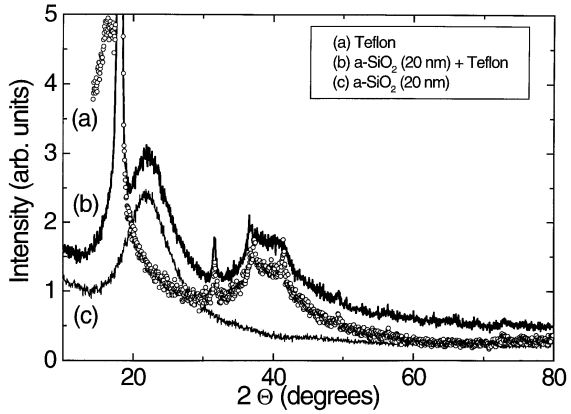


**Fig. 1.** X-ray diffraction patterns for the: Teflon powder (sample S9, curve (a)), amorphous 20 nm $SiO_2$ grains (as-received, curve (c)), and the pressed mixture (sample S1, curve (b)). The intensity of each curve has been arbitrarily scaled to facilitate comparison.

## 3 Experimental details

### 3.1 Sample characteristics

For our measurements we have used commercially available amorphous and crystalline $SiO_2$ powders. The samples S1, S2 and S3 were prepared with vitreous silica a-$SiO_2$ powders with typical size of 4 nm and 20 nm [8], see Table 1. The powders were supplied as a water dispersion. The water has been removed by vacuum drying before the measurements.

Figure 1 shows the X-rays diffraction pattern taken from the 20 nm powder alone (curve (c)). We clearly see the typical amorphous halo. We stress that crystallites of 20 nm size would not produce this kind of pattern, but clear discernible diffraction peaks with an average width FWHM $< 1$ degree.

For the measurements in the calorimeter the powders were mixed with Teflon powder (typical particle size 6–9 $\mu$m [9]) and pressed ($p = 1200$ bar) into a Teflon container (diameter 2 cm, thickness 0.1 cm, length 2–4 cm). The mass fraction $\alpha$ of $SiO_2$ in the mixture with the Teflon powder was 50% for samples S1 and S2, whereas $\alpha \simeq 14\%$ for sample S3.

The mixture and press procedure has been carried out at atmospheric conditions; thus, from the preparation it cannot be excluded that some rest gas (oxygen and nitrogen) remained in the samples. However, we can estimate the free volume for these gases for the different samples and we found that there is *no correlation* of this volume with the observed experimental anomalies, although the density of the samples has been varied by nearly 80% up to the density of Teflon ($\rho \simeq 2.2$ g/cm$^3$). We have chosen Teflon as matrix because its heat release is small (see below) and, at the temperatures of our measurements, it provides good thermal coupling and a thermal diffusion time appropriate to our purposes.

In Figure 1 we show also the X-ray patterns of the pressed powder with Teflon and of Teflon alone. It should be noted that the used Teflon is not completely amorphous but consists of approximately 50% crystalline portion. Teflon as well as the a-$SiO_2$ powders do not change basically their X-ray patterns after pressing them, see Figure 1.

The samples S4 to S8 were prepared by mixing the Teflon powder with a crystalline quartz powder. The as-received powder was 99.5% $SiO_2$ [10] with a typical particle size of 20 $\pm$ 10 $\mu$m [11], samples S4 and S5. The particle size of this quartz powder was further reduced by ball milling to 5 $\pm$ 3 $\mu$m (3 h milling, sample S6) and 1 $\pm$ 0.5 $\mu$m (12 h milling, samples S7 and S8). These are the mean particle sizes of the grains with the largest contribution to the volume of the sample. Our measurements of the grain size distribution show that a non negligible number of grains have smaller size (a factor five to ten smaller).

Figure 2a shows the X-ray diffraction pattern of the as-received 20 $\mu$m quartz powder alone (unpressed) and the pressed mixture with Teflon. From the X-ray pattern, we note that the as-received grains of the quartz powder are of very good crystalline quality. The relative small FWHM of the X-ray peaks and the clear splitting due to the Cu-K$\alpha$ radiation for the peak at $2\theta \simeq 36.6°$, for example (see Fig. 2b), indicate that the crystallites have a negligible amount of lattice distortions or lattice defects.

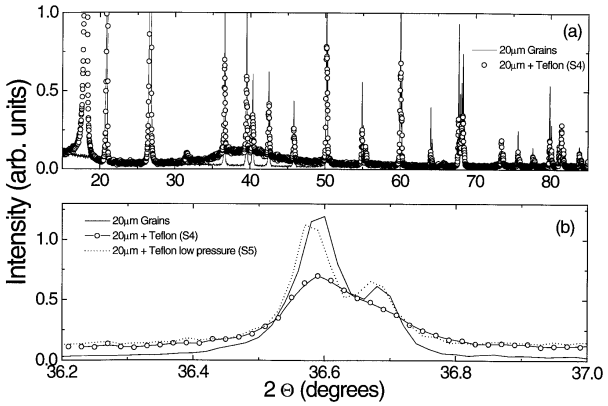


**Fig. 2.** (a) X-ray diffraction patterns for the crystalline 20 $\mu$m $SiO_2$ powder (as-received) and the pressed mixture with Teflon (sample S4). (b) Part of the pattern around 36.6° for the same samples as in (a) including sample S5.

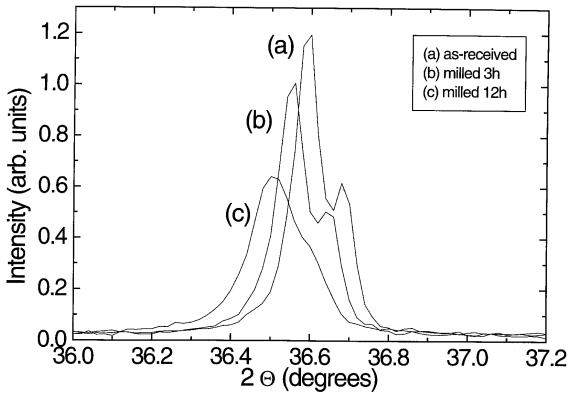


**Fig. 3.** X-ray diffraction patterns around 36.6° for the crystalline 20 $\mu$m $SiO_2$ powder (as-received), curve (a), and for the 5 $\mu$m (curve (b)) and 1 $\mu$m (curve (c)) powders obtained by ball-milling.

After pressing the quartz powder with Teflon (sample S4), the crystallites reveal a clear enhancement of the FWHM due to lattice deformation, see Figure 2b. In the same figure we show the diffraction peak for the same as-received quartz powder but pressed with the Teflon powder using 30 times lower pressure (40 bars, sample S5). Within the resolution of our X-rays diffractometer (X'pert from Phillips) no remarkable difference in the FWHM can be recognized between the quartz powder alone and that from sample S5.

Micrographs of different parts of the pressed quartz samples (S4–S8) reveal that the grains are embedded completely by Teflon without any sign of cluster formation. Micrographs from samples S1–S3 reveal a rather homogeneous "paste", in which the nm small grains cannot be recognize due to the resolution limit of the scanning microscope.

As expected, milling introduces defects in the atomic lattice of the quartz grains, in addition to those produced by the high pressure used for pressing the mixture. This is clearly seen from the enhancement of the width of the diffraction peak at 36.6°, see Figure 3.

The Vycor sample [12] has a porosity of 30% and an average pore radius $\sim 3 \ldots 4$ nm [13]. The surface to mass ratio is $\simeq 100$ m$^2$/g. Three cylinders with a diameter of 18 mm have been cut from a 1 cm thick Vycor sheet and put into a fitting Teflon container which has been closed under vacuum at room temperature to avoid gas inclusion.

### 3.2 Experimental methods

According to the standard tunneling model both properties, the specific heat $C(T)$ and the heat release per sample volume $\dot{Q} = \mathrm{d}Q/\mathrm{d}t$, are proportional to the density of states of the low-energy excitations $P_0$ according to the relations which hold for $\tau_{min} \ll t < \tau_{min}/u^2_{min} \sim 10^{10}$ s at $T \leq 1$ K (see for example Refs. [14–16])

$$C \simeq (\pi^2/12) k_B^2 T P_0 \ln(66.24 A T^3 t), \qquad (7)$$

derived taking into account the dominant phonons only [17], and

$$\dot{Q} \simeq \frac{\pi^2}{24} k_{\mathrm{B}}^2 P_0 \left(T_1^2 - T^2\right) \frac{1}{t} \cdot \qquad (8)$$

The parameter $u_{min} < 10^{-9}$ is introduced as a cutoff to keep the number of TS finite; $T_1$ is the "charging" or equilibrium temperature of the sample before cooling to the measuring temperature $T$ and $t$ is the time; $A \simeq 8.5 \times 10^7$ s$^{-1}$K$^{-3}/k_B^3 \propto \gamma^2$ is a parameter that depends on the coupling constant $\gamma$ between phonons and TS.

We should stress that equation (8) usually applies for charging temperatures $T_1 \leq 2$ K [15]. At higher charging temperatures, high order processes and/or thermally activated relaxation overwhelm the tunneling mechanism. In this case and at high enough $T_1$ the heat release saturates as a function of $T_1$ [15,16].

If the theory of interacting TLS were correct, the density of states $P_0$ should be influenced by the particle size and we could hope to find an effect on both properties. Note that in the time and temperature scale of our experiments the heat release is the only property that allows a direct measurement of the density of states of TS without any free parameter, in contrast to the specific heat where the value of the averaged coupling constant between TS and phonons is needed, see equation (7). At longer times, however, both properties depend on the value of $u_{min}$ [14,16], *i.e.* the finite number of TS produces a downward deviation from the $1/t$ dependence in $\dot{Q}$. The possibility of using the heat release at very long times to obtain an estimate of the parameter $u_{min}$ has been discussed in references [14,16]. The soft potential model and for long enough times $t \gg \tau_{min}$ predicts a slightly different time dependence for $\dot{Q}$ as that given by equation (8), *i.e.* $1/t \to 1/[t \ln^{2/3}(t/\tau_{min})]$ [18]. Precise heat release measurements over 3 to 4 decades in time would be necessary to distinguish between the time dependencies predicted by the models. For our purposes, we restrict ourselves to the use of the standard expression (8).

For both kinds of measurements, the specific heat and the heat release, we have used the same experimental setup. The specific heat was measured when the heat release was negligible. The workable temperature range for the specific heat measurements was 0.1–1 K. The specific heat was measured mostly with a semi adiabatic heat pulse technique. The time dependence of the sample temperature after application of the heat pulse follows an exponential decay which can be fitted with a single time constant in the temperature range reported in this work. All the measurements of the specific heat as well as the time response of the system indicate that the thermal diffusion time within the sample was shorter than the one measured between sample and bath. An example of the time dependence of the sample temperature at and after the application of the heat pulse is given in the inset of Figure 6, see below. A similar time dependence within and after applying the heat pulse has been observed for samples prepared with different pressures. If part of the embedded grains would be poorly thermally coupled to the Teflon, the results obtained here would provide a lower limit for the specific heat of the small grain systems.

All the heat release measurements have been carried out at a measuring temperature of $T$= 200 mK. For more details on the heat release method and its experimental setup see reference [15]. The long-time stability of the mixing chamber temperature was better than 0.15 mK. As thermometer two previously calibrated $RuO_2$ thin film resistors [19] were used. The measurements have been carried out in a top-loading $^3$He/$^4$He dilution refrigerator.

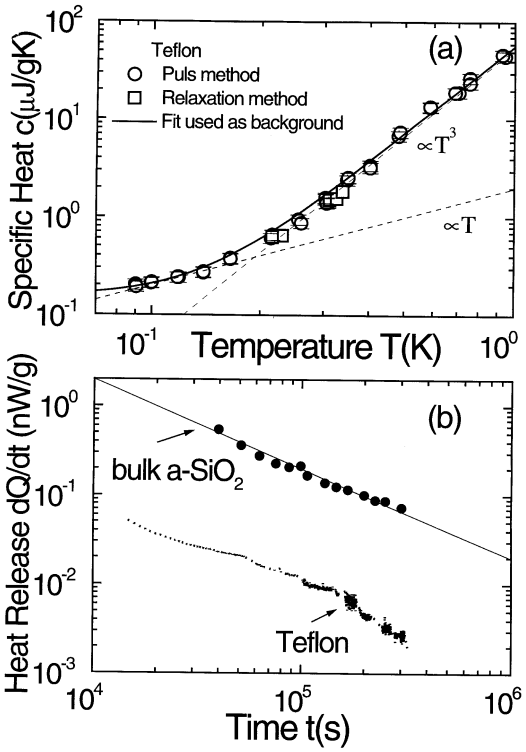


**Fig. 4.** (a) Specific heat of the pressed Teflon powder including the Teflon sample holder, as a function of temperature, obtained using relaxation and puls methods. The straight dashed lines follow a $T^3$ and $T$ dependence. The solid line is a fit of the experimental data, that was used as a background line to be subtracted from the measurements of the specific heat of the composites. (b) Heat release as a function of time for Teflon (lower curve) and for bulk a-$SiO_2$ (close circles taken from Ref. [20], upper curve) for a charging temperature $T_1 = 80$ K measured at $T = 0.2$ K. The straight line follows a $t^{-1}$-dependence.

## 4 Experimental results

### 4.1 Teflon

As mentioned above, we have selected Teflon as sample holder as well as the medium for the thermal contact between the vitreous silica (or quartz) grains. The specific heat and heat release of Teflon (sample S9, see Tab. 1) are shown in Figure 4. For comparison we show also in Figure 4b the corresponding results for bulk a-$SiO_2$ (Suprasil W) taken from [20]. The specific heat of Teflon shows a $T^3$ dependence down to 300 mK, see Figure 4a. The deviation from this law is due to the contribution of TS given by an additive linear term. As expected, this contribution is smaller than for a-$SiO_2$, because the Teflon sample was not completely amorphous as shown by X-ray diffraction, see Figure 1. The contribution of Teflon, considered as background, has been subtracted from the measurements described below. Because the overall specific heat of Teflon is larger than of a-$SiO_2$, this subtraction diminishes the resolution for the determination of the specific heat of the composites, specially at $T \sim 1$ K.

The reason for using Teflon as binding matrix becomes clear from the results of the heat release shown in Figure 4b. The heat release of Teflon measured at $T$ = 200 mK and after cooling for a charging temperature $T_1$ = 80 K is much smaller than for bulk a-$SiO_2$. This small heat release allows a precise measurement of the heat release of the composites, when the mass fraction $\alpha$ is not so small, *i.e.* $\alpha > 20\%$. Assuming that the ratio $\dot{Q}(t = 10^4\,\mathrm{s}, T_1 = 1\,\mathrm{K})/\dot{Q}(t = 10^4\,\mathrm{s}, T_1 = 80\,\mathrm{K}) \simeq 5{\times}10^{-4}$ measured for bulk a-$SiO_2$, applies also for Teflon, then we would have a heat release $\dot{Q}(t \geq 10^4\ \mathrm{s}) < 10^{-4}$ nW/g, which is below the resolution limit of our measuring system.

### 4.2 Amorphous $SiO_2$ grains embedded in Teflon

Figure 5 shows the heat release of the composites 20 nm and 4 nm a-$SiO_2$ grains with Teflon, samples S1 to S3, as a function of time for two charging temperatures. Due to the small a-$SiO_2$ mass in sample S3, it was not possible to measure its heat release for $T_1 = 1$ K. All the data shown in Figure 5 and of samples with $SiO_2$ grains (amorphous or crystalline) shown below are normalized by the mass of the $SiO_2$ grains *only*. The contribution of the Teflon

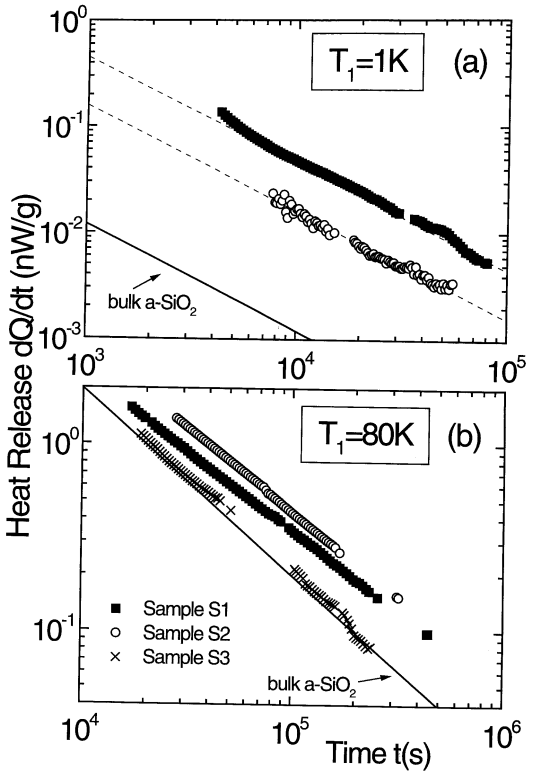


**Fig. 5.** (a) Heat release as a function of time for a charging temperature $T_1 = 1$ K measured at $T = 0.2$ K for sample S1 and S2. The dashed lines follow a $t^{-1}$ dependence, as well as the continuous line below obtained for bulk a-$SiO_2$ [20]. (b) The same as (a) but for a charging temperature $T_1 = 80$ K and including the results for sample S3. The straight line indicates the heat release obtained for bulk a-$SiO_2$.

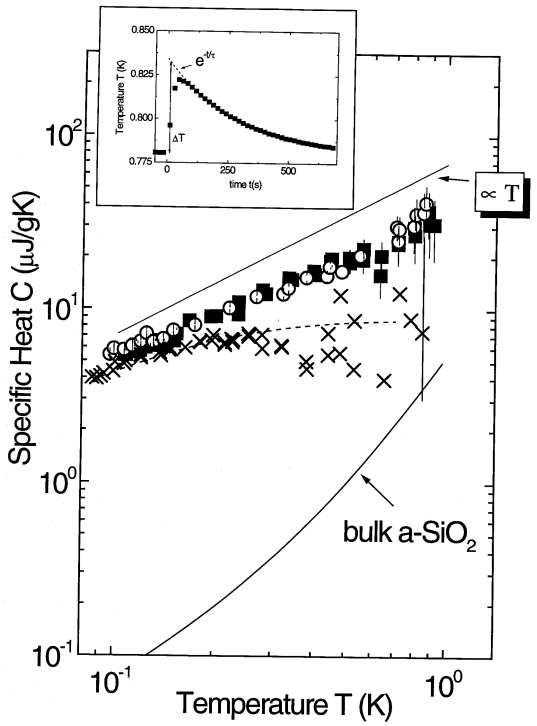


**Fig. 6.** Temperature dependence of the specific heat of a-$SiO_2$ grains with 4 nm and 20 nm particle sizes. The contribution of the Teflon matrix and sample holder was subtracted and only the mass of the grains was taken into account. (■): Sample S1, (○): sample S2, (×): sample S3, the dashed line is only a guide to the eye. The upper straight line follows a linear temperature dependence. The lower continuous line represents the results for bulk a-$SiO_2$ (Suprasil W data taken from [21]). The inset at the upper part of the figure shows the time dependence of the sample (S1) temperature at and after the application of the heat pulse. The temperature after the heat pulse follows an exponential decay law with a single relaxation time $\tau$.

matrix and sample holder to the specific heat and heat release has been always subtracted with exception of the data of the heat release at $T_1 = 1$ K, where their contribution has been considered as negligible, as follows from the measurements of sample S9. We note that the heat release for samples S1 and S2 and for $T_1 = 1$ K is much larger (up to 40 times) than for bulk a-$SiO_2$.

Figure 6 shows the specific heat as a function of temperature for the samples S1 to S3. We found a strong increase of the specific heat below 1 K in comparison to bulk a-$SiO_2$. For these samples the specific heat is up to 50 times larger than for bulk a-$SiO_2$ at the lowest temperatures. Note that although similar specific heat has been measured for samples S1 and S2, a difference is observed in the heat release, see Figures 5a and 5b. Moreover, the difference between the two samples is qualitative different, *i.e.* sample S1 shows a three times larger heat release than S2 for $T_1 = 1$ K but it is 30% smaller for $T_1 = 80$ K. This difference can be ascribed, at least partially, to the difference of charging time used for sample S2: 10 h in comparison with 24 h charging at $T_1 = 80$ K used for sample S1. Another possibility to interpret this difference may be related with the actual grain distribution. Although the nominally 20 and 4 nm average grain size provided by the company may be correct, it cannot be ruled out that their distributions may overlap. According to our measurements, the reproducibility of the heat release results for samples prepared under similar conditions and with the same powder is within the scattering of the data.

From the measurement of the heat release we have the possibility to check the contribution due to tunneling systems to the thermodynamic properties. We know that at the charging temperature of 1 K equation (8) applies [15,16]. Indeed, the samples show approximately the predicted $1/t$ dependence for the heat release (see Eq. (8)). Furthermore, the density of states $P_0$ obtained from these measurements is similar to that deduced from the specific heat. The calculated density of states $P_0$ is shown in Figure 7 as a function of the average radius of the $SiO_2$ grains. The measured $t$- and $T$-dependence of the heat release and specific heat and the similar density of states calculated from these properties indicate that the anomalies are due to the contribution of tunneling systems. The obtained density of states for these samples is strongly enhanced in comparison with bulk a-$SiO_2$, see Figure 7, indicating a clear deviation from the universality of $P_0$ observed for bulk amorphous and disordered systems.

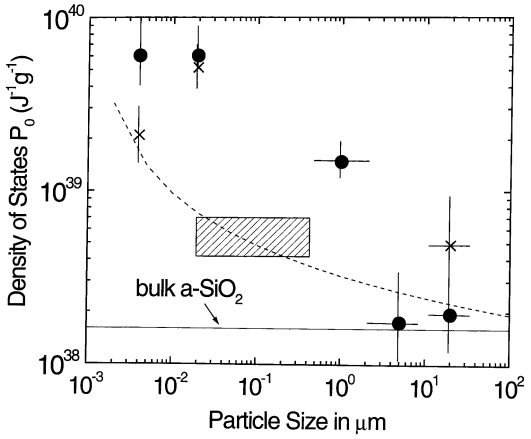


**Fig. 7.** Density of states of tunneling systems $P_0$ as a function of the typical particle size, calculated from the approximately linear temperature contribution to the specific heat (•, using Eq. (7) with the same value of the parameter $A$ and with $t =$ 10 s), and from the time dependence of the heat release at $T = 200$ mK with a charging temperature $T_1 = 1$ K (×). The samples with 20 nm and 20 $\mu$m grain size were charged 24 hs, the sample with 4 nm grain size only 10 hs. This may reduce the density of states obtained from the heat release measurements in comparison with the value obtained from the specific heat. The dashed area denotes the values obtained from a-$SiO_2$ thin films from [4]; the width of this area is the error in the determination of $P_0$ from the slope of the sound velocity. The dashed line is given by $P_0 = 2.2 \times 10^{39}$ [1/Jg]/ $\ln(10^4 R)$, where $R$ is the grain size in $\mu$m.

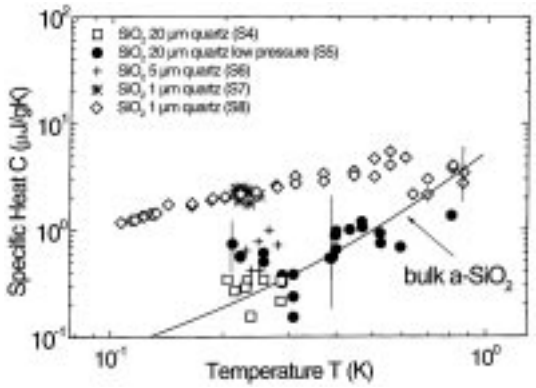


**Fig. 8.** Specific heat as a function of temperature for sample S5 (20 $\mu$m quartz grains embedded in Teflon pressed with low pressure, (•)) and sample S8 (1 $\mu$m quartz grains (◇)). We include also the results of the specific heat obtained for samples S4, S6 and S7. The continuous line is obtained for bulk a-$SiO_2$. As always, the contribution of the Teflon matrix and sample holder was subtracted and only the mass of the grains was taken into account.

If we neglect any strain interaction between the grains through the Teflon matrix, we would expect that $P_0$ remains unchanged as a function of the distance between a-$SiO_2$ grains. In Figures 5b and 6 we show the results obtained for sample S3, that was prepared with the 20 nm grains with a weight ratio between $SiO_2$ and Teflon $\alpha \simeq 14$ %, We observe that both properties show clear changes, indicating that the density of states of low-energy excitations tend to decrease in comparison with samples S1 and S2. Note also that the $T$-dependence of the specific heat deviates from a simple linear dependence as observed for samples S1 and S2 and for vitreous silica. A discussion of these and other results will be given in the next section. In the next subsection we present the data of composites prepared with quartz powder (samples S4–S8).

### 4.3 Quartz grains embedded in Teflon

According to the published literature, crystalline bulk $SiO_2$ without any irradiation, shows no or negligible evidence for low-energy excitations. To the best of our knowledge, thermodynamic properties of quartz samples with dimension in the micrometer range have not been reported yet. As we shall discuss in the next section, a lettered reader may tend to correlate the rather extraordinary increase of the specific heat decreasing the grain size with, for example, a fracton contribution as found in aerogels (see for example [22,23]). One may also tend to correlate the observed effects in the composites to surface contribution at the grains, or to an intermediate layer in the Teflon and between the $SiO_2$-grains. The measurements on small quartz particles shown below and, in the next section, on Vycor were stimulated from those speculations. As we will see below, the results with quartz particles clarify only partially these open issues.

Figure 8 shows the temperature dependence of the specific heat for the samples S5, S7 and S8. For the samples S4 and S6, data were taken only in the temperature range 0.2 K to 0.3 K. Within the error, the data for samples S4 and S5 coincide with the curve measured for bulk a-$SiO_2$, whereas samples S6, S7 and S8 show a larger specific heat. In order to assure that this anomalous large specific heat (for quartz) is due to the contribution of TS, we have measured the heat release for samples S4 and S5, see Figure 9a. At a charging temperature $T_1 = 1$ K only tunneling relaxation is important, therefore any difference observed between the heat release of different samples can be related directly to a change in the density of states of TS, see equation (8). In good agreement with the specific heat results (see Fig. 8) the 20 $\mu$m quartz grains embedded in Teflon (sample S4) indicate similar density of states of TS as bulk a-$SiO_2$.

Decreasing the size of the quartz particles by ball milling to an average of 1 $\mu$m (samples S7 and S8), the specific heat increases in our temperature range and shows a temperature dependence similar to that obtained for sample S3, compare Figures 6 and 8.

All the samples discussed above were prepared by applying a pressure of 1200 bar to compact the composite. Taking into account the well-known contribution of fractons to the specific heat of aerogels [22,23], we have performed measurements on a composite sample prepared applying much less pressure. If the specific heat of a composite increases due to a fracton contribution, the heat release should not change since according to

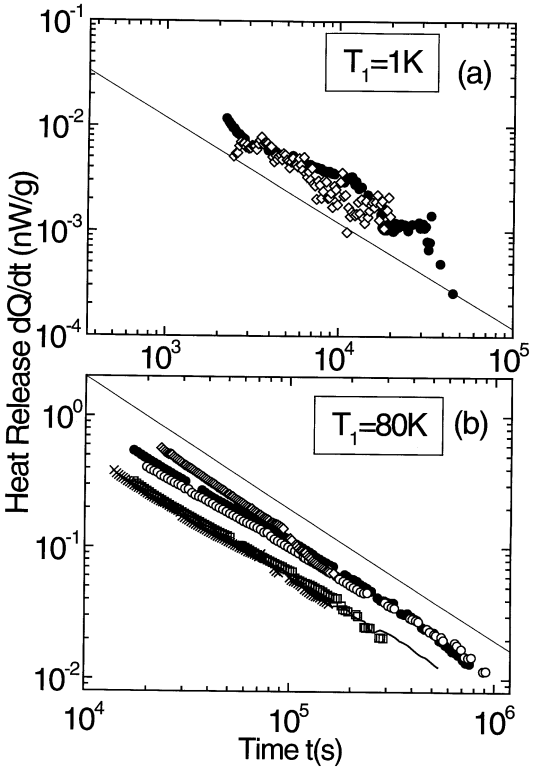


**Fig. 9.** (a) Heat release as a function of time for a charging temperature $T_1 = 1$ K measured at $T = 0.2$ K for the quartz samples S4 (•) and S5 (◇). The straight line follows a $t^{-1}$ dependence and corresponds to bulk a-$SiO_2$. (b) The same as (a) but for a charging temperature $T_1 = 80$ K and for samples S6 (○), S7 (×, □) and S8 (−). The heat release of sample S7 was measured twice at different runs to check for the reproducibility of our measurements. The straight line indicates the heat release obtained for bulk a-$SiO_2$.

our assumptions, it is only due to the relaxation of TS. For this purpose we have prepared sample S5, using the same quartz powder as for sample S4 but applying 30 times less pressure. The results are shown in Figures 8 and 9a. Due to the relative smaller amount of $SiO_2$ powder in sample S5 and the large specific heat of the Teflon matrix, the specific heat data of sample S5 have a large error, see Figure 8. We tend to conclude, nevertheless, that the specific heat of the low pressured sample S5 remains similar to sample S4 and to bulk a-$SiO_2$. The heat release, also, does not change within the error, see Figure 9a. This result indicates that lowering the density of the sample by applying less pressure, no additional excitations contribute to the specific heat or to the heat release.

The heat release for different quartz grains (samples S4 to S8) and for a charging temperature $T_1 = 80$ K is shown in Figure 9b. We observe that the heat release for samples S4 and S6 is smaller by a factor of two than for bulk a-$SiO_2$, and it is even smaller for the 1 $\mu$m quartz grain (samples S7 and S8). Note that the heat release with charging temperature $T_1 = 80$ K is smaller the smaller the quartz particle, whereas the specific heat increases, compare Figures 8 and 9b. We should stress again that at

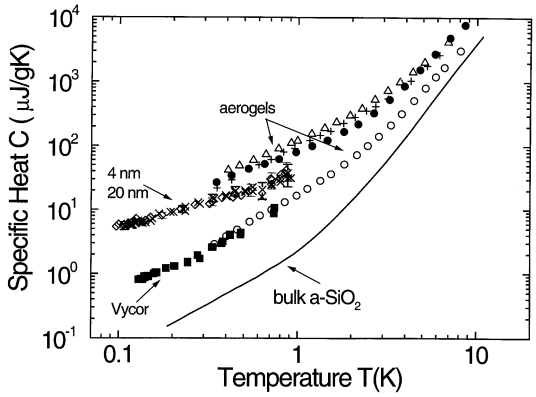


**Fig. 10.** Specific heat as a function of temperature for Vycor (■), (◇): sample S1, (×): sample S2. Taken from reference [22] we show the data of the samples: (○): BC 0.87, (•): BC 0.27, (+): A-NC 0.36, (△): A-NC 0.12. The continuous line corresponds to the specific heat for bulk a-$SiO_2$.

charging temperatures $T_1 > 5$ K no simple correlation between $\dot{Q}$ and $P_0$ can be assumed due to the contribution of high-order relaxation processes of the low-energy excitations and the influence of the cooling procedure [15,16]. Nevertheless, the data obtained for the quartz grains indicate indeed a surprisingly similar distribution of energy and relaxation time as for bulk a-$SiO_2$.

### 4.4 Vycor

A way to clarify if Teflon and/or of a Teflon layer between the grains has a significant contribution to the observed anomalies, is given by the measurements on Vycor. Due to its low density and porous medium, it can be expected that if TS (and not "fractons") provide the main contribution to the thermodynamic properties of the composite, an enhancement of $\dot{Q}$ and $C$ relative to bulk a-$SiO_2$ should also be observed.

A large enhancement of the specific heat (of the order of 100), as observed for our smaller amorphous grains, has been observed in silica aerogels [22,23]. These samples have a mass density at least ten times smaller than for bulk a-$SiO_2$. de Goer *et al.* [22] interpreted these data in terms of fractal networks. They concluded [22], however, that in silica aerogels tunneling systems cannot be the origin of the enhancement of the specific heat.

For the small density aerogels and taking into account the available volume of these samples and in our arrangement, it is not possible for us to accurately measure the heat release of similar aerogels. Therefore, we have chosen Vycor for these studies.

Figure 10 shows the temperature dependence of the specific heat of Vycor (sample V1). The specific heat is larger than for bulk a-$SiO_2$ by a factor of ten and coincides with that measured for sample BC 0.87 from [22] at $T >$ 0.3 K, see Figure 10. For comparison we show in the same figure the specific heat data for the samples S1 and S2 and for the low-density aerogels taken from [22]. Taking into account the common interpretation of the specific heat in

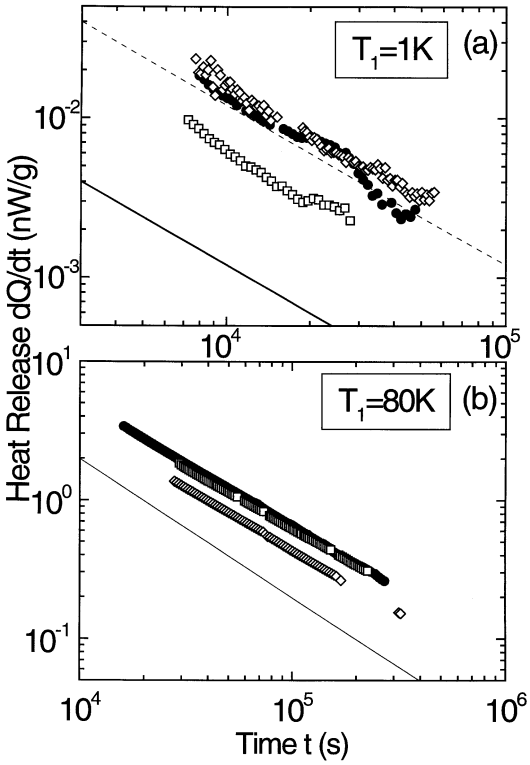


**Fig. 11.** Heat release as a function of time at $T = 0.2$ K for Vycor obtained charging the sample at a temperature $T_1 = 1$ K for 24 hs (•), 15 min (□), and of sample S2 (◇). The dashed line follows a $t^{-1}$ dependence. The straight line is the heat release for bulk a-$SiO_2$. (b) The same as (a) but for a charging temperature $T_1 = 80$ K for Vycor (□, •) and for sample S2 (◇). The straight line is the heat release for bulk a-$SiO_2$.

low density silica samples [22] one would tend to conclude that in Vycor other kind of excitations like fractons may contribute to the specific heat.

However, the heat release clearly indicates that the contribution of TS is not negligible. Figure 11 shows the heat release at $T = 200$ mK for two charging temperatures $T_1 = 1$ K and $T_1 = 80$ K. For $T_1 = 80$ K, the heat release of Vycor is larger than for bulk a-$SiO_2$ by a factor two and shows a $1/t$ dependence, as expected from the tunneling model with a broad distribution of TS-energies and relaxation times. Note that the heat release of Vycor is larger than for all the other measured samples, see Figure 11b.

Charging sample V1 at $T_1 = 1$ K, the heat release follows a $1/t$-dependence at $t > 7 \times 10^3$ s, being 10 times larger than for bulk a-$SiO_2$, see Figure 11a, in very good agreement with the specific heat indicating an enhanced density of states of TS. Certainly, this result casts some doubts on the interpretation of the enhancement of the specific heat in terms of fractal-like excitations. A further support for a TS contribution to $\dot{Q}$ is provided by its dependence with the charging time. As seen in Figure 11a, $\dot{Q}$ decreases decreasing the charging time, as we would expect from the tunneling model.

## 5 Discussion

The discussion is organized in two parts. In the next section we discuss the obtained results within the predictions of the interaction theory from Burin and Kagan [3] assuming a sample size dependence of the density of states of TS. The results obtained for the quartz grains embedded in Teflon reveal a more complicated picture than the simple one presented in the first part. Therefore, the role of surface defects as well as Teflon will be discussed in the second part of the discussion, taking into account the results of Vycor.

### 5.1 Sample size dependence of the density states of TS

The stability requirement for the low-energy state considered for the first time by Efros and Shklovskii [24] ensures the universal dependence of the density of states on the system size at sufficiently low temperatures. For a $1/R^3$ interaction this dependence is logarithmic (see Eq. (5)) if the system size is larger than some intermediate length $L_*$.

Let us discuss the experimental data from this point of view. The decrease of the density of states of excitations with increasing grain size agrees with theoretical pictures based on the long-range interaction between some initial entities with internal degrees of freedom. For the dependence of that spectral density $P_0$ on the grain size (see Fig. 7) Burin-Kagan theory predicts a logarithmic behavior. However, and within the scattering of the data, the nearly two orders of magnitude difference between the $P_0$ for the bulk sample and for the small amorphous grains can not be simply explained by the weak logarithmic factor, see Figure 7.

A source for the large increase of the density of states can be the polydispersion of grains. The fraction of grains with size $L < L_*$ may have a larger density of excitations and contribute significantly. Note also that the effect of correlations between various grains may complicate the expected dependence because the concentration of grains is rather high and some may touch each other. This and polydispersion may have also an influence on the temperature dependence of the specific heat: Note the deviation from the linear temperature dependence in Figure 6, as well as the larger heat release obtained for the 20 nm grains at $T_1 = 1$ K, see Figure 5a. In future experiments the discrimination between various mechanisms should be solved using perhaps mono dispersive grains with smaller concentration, so that the correlations between them can be neglected. In the absence of correlations the heat capacity as well as the heat release should increase linearly with the number of grains.

Note also, that the apparent decrease of $P_0$ decreasing the density of a-$SiO_2$ grains in Teflon (sample S3) seems to contradict the simple expectation based on the interaction theory: A larger distance between grains should increase $P_0$ if the interaction between TS from different grains plays the main role. Certainly, the presence of

Teflon for the latter sample can modify the interaction constant $U_0$. Strictly speaking a decrease of $U_0$ can be expected since Teflon is softer than $SiO_2$ and the density of acoustic phonons in $SiO_2$ grains might be reduced.

Recently published measurements of the sound velocity of thin a-$SiO_2$ films at very low temperatures show a slightly larger quasi-logarithmic slope as a function of temperature as for bulk a-$SiO_2$ [4]. These data may indicate that the thickness of those films influences the density of states $P_0$, assuming that the increase of the slope of the sound velocity (proportional to the product $P_0\gamma^2$) is due to a change in $P_0$. These results are enclosed in the shaded area of Figure 7, where the height of the area represents the error in the determination of the slope.

At this stage of the discussion we may conclude, therefore, that the enhancement of the specific heat is apparently caused by a variation of the density of states of the tunneling systems with the sample size characterized by the typical diameter of the samples, and that this enhancement may be understood qualitatively within the Burin-Kagan theory [3]. However, several questions remain open, as for example: (a) in amorphous grains as small as 4 nm, can one still assume to have a large enough number of TS within the grain that allow the application of the Burin-Kagan theory? (b) Why the mixture of small quartz grains with Teflon shows similar or even larger heat release and specific heat as bulk a-$SiO_2$? Evidently the contribution of the surface of the grains and/or Teflon should be carefully taken into account before an interpretation for the observed sample size dependence of the measured low-temperature properties is given. This is discussed in the next section.

### 5.2 Contribution of Teflon and surface effects to the measured properties

Besides the striking increase of the density of states of TS in small amorphous grains of $SiO_2$ observed by the heat release and specific heat, the second and surprising result of this work is related to the glass-like thermodynamic properties of the micrometer large crystalline $SiO_2$ grains depicted in Figures 8 and 9.

It is tempting to correlate the glass-like properties of the quartz grains to a large number of defects of the grains. This does not seem quite plausible if we take into account the X-ray data. From the results shown in Figures 2 and 3, specially the K$\alpha$-splitting of the peak observed at 36.6° and the relatively small FWHM, we conclude that the 20 $\mu$m quartz powder consists of almost perfect crystallites with negligible amount of defects in their crystalline structure.

One may also argue that the high pressure used to prepare the composite produces enough distortion of the lattice and therefore generating tunneling defects, see the X-ray data in Figure 2b, similar to the generation of defects due to ball milling as observed by the increase of the FWHM in Figure 3. However, the thermodynamic data do not support this interpretation: The 20 $\mu$m quartz powder embedded in Teflon with high (sample S4) and low pressure (sample S5) shows, however, similar specific heat, see Figure 8, and heat release, see Figure 9a.

What about the contribution of Teflon in the composite? We have shown that Teflon alone and pressed with the same procedure as for the composites, does show a much smaller heat release than all other measured samples, see Figure 4b. Also the possibility that the degree of polycrystallinity of Teflon is changed due to the mixing with the powders is not supported by the X-ray data, see Figures 1 and 2a. The large increase of the heat release of Vycor in comparison with bulk a-$SiO_2$, an increase of the order of that observed for the composites, see Figure 11, clearly indicate that Teflon cannot be the reason for the larger density of states of TS in the amorphous grains as well as for the glass-like thermodynamic properties of the quartz grains. The comparison of the results of Vycor and the samples S4 and S5 indicates that a composite prepared with low density (*i.e.* at relatively lower pressure) does not seem to show contributions from other excitations than TS in the specific heat and heat release, see Figures 8, 9a, and 10. From all these results we would conclude that a "special" Teflon layer between the grains is probably not the cause for the anomalies we observe.

A probable cause for the glass-like low-temperature properties of the quartz grains, as well as for the enhancement observed for the amorphous powder, may be attributed to the contribution of defects at the surface of the grains.

The contribution of the properties of the surface of the grains should be even more important the smaller their dimension. Then, one may believe that this would increase the density of states of TS. It is nevertheless surprising that the quartz grains show quantitatively similar values of $P_0$ as bulk a-$SiO_2$ or even larger (sample S7). We believe that the interactions between the defects should also play a main role in the crystalline samples in order to achieve similar values of $P_0$ (as well similar $T$- and $t$-dependence of the specific heat and heat release).

The increase of the density of states of TS with the relative increase of the internal surface may be not necessarily due to an increase of the defect density itself, but to a change in the dimensionality of the interaction for those surface defects. The arguments used in the last section to try to explain the increase of $P_0$ by the decrease of the interaction radius $R$ would be here also applicable. It should be noted, that a correlation between density of states and sample surface is implicitly included in the behavior shown in Figure 7 if we plot it as a function of the ratio of the sample mass to surface ($\propto R$). In this case also the results of Vycor would support this dependence using the ratio of 0.01 g/m$^2$.

Finally, we would like to discuss briefly the results with high charging temperature leaving by side the question on the nature of the TS in the quartz grains discussed above. In Figures 5b and 9b we have shown the long-time heat release with high charging temperatures ($T_1 = 80$ K). It is well-known that the low-temperature heat release in this case is mainly determined by high-order relaxation

processes (*e.g.* thermal activation) which relax the TS at relatively high temperatures ($T \geq 5$ K) during the cooling down procedure [15]. We find that in all samples the time dependence of the heat release is slightly weaker than the $t^{-1}$-dependence predicted by the tunneling model. However, this has been found also in bulk samples and is of minor interest for our present investigations. The interesting conclusion we can draw from these measurements is that the sample dimension influences the high-order processes. This can be deduced mainly from the composite with 1 $\mu$m quartz grains (samples S7 and S8) that show a heat release that is *half* the value of a bulk sample, see Figure 9b, but has a specific heat at $T \leq 200$ mK nearly ten times *larger* than for bulk a-$SiO_2$, see Figure 8. Additionally, for all samples the variation of the heat release with sample size and high charging temperatures is weaker than the variation of the specific heat, which also indicates that the sample size has an influence on the relaxation processes above 1 K.

According to theory, the increase of the interaction radius with decreasing temperature leads to the formation of complex TS containing many defects [3,25]. They have very large relaxation times which increase exponentially with increasing the number of defects. The density of TS containing a small number of defects as well as the total density of TS decreases in accordance with the dipole gap theory so that the heat capacity always decreases with increasing the effective size $L$. Therefore, one expects an increase of the density of TS having a *larger relaxation time* increasing the size $L$, which ensures a larger heat release. This observation would allow us to interpret the behavior of the heat release and heat capacity for the 1 $\mu$m grains sample, which shows smaller heat release as the larger quartz grains.

## 6 Conclusion

Concluding, we have measured the specific heat and heat release of small grains of amorphous and crystalline $SiO_2$ and of Vycor. We have found a strong influence of the sample dimensions on both properties. The strong enhancement of the specific heat and heat release decreasing the particle size appears to be in qualitative agreement with the framework of the Burin-Kagan theory of strongly interacting tunneling systems. However, the unexpected results of the glass-like anomalies in quartz grains point out that probably surface defects and their interaction may play a mayor role in this enhancement. The heat release results for Vycor clearly show that the contribution of TS is large.

Heat release measurements with high charging temperatures ($T_1 = 80$ K) demonstrate the influence of the particle size on the relaxation processes relevant during the cool down of the sample. Although the interpretation for the influence of the average distance between particles is not yet completely understood, our results show the wide applicability of the small particle system.

The experimental data demonstrates that the number of two-level excitations can be verified experimentally in the materials composed from powders of micro or nano size particles. Note that in bulk amorphous solids the density of TLS is sensitive to the melting or annealing temperature (see [26] and references therein). One should note that recent experimental data [27] proves that the number of TLS can be lowered in thin films of a-$SiO_2$ by preparation in hydrogen atmosphere. Thus, all these and our results show that the problem of control the number of the strongly anharmonic excitations like TLS can be resolved by using systems of reduced dimensionality or size. On the other hand, a comparison of the results on amorphous thin films [4,28,29] with those obtained on grains is not straightforward. In spite of the fact that the slight increase of $P_0$ deduced from the sound velocity data obtained in reference [4] appears to agree with the theoretical expectations, see Figure 7, we note that: The interaction at distances less than the film thickness would be defined by three dimensional phonons and behaves as $U_0/R^3$, whereas at larger distances it is defined by two-dimensional phonons and decreases as $U_0/LR^2$. The interaction $1/R^2$ is long range and would provide similar TS-properties (like $P_0$) as observed for the bulk samples, with exception of the energy dependence of the relaxation rate of TS because of the change in the phonon spectrum [4]. Therefore, isolated grains of small dimensions are preferable systems to test the prediction of the interaction theory.

Two-level excitations have in general an anharmonic nature [30]. They influence the internal friction in a wide temperature range up to several hundreds degrees where the character of their motion changes from tunneling to thermally activated. Since the internal friction especially near the surface is closely connected with the sliding friction [31] we would expect that the implications of our work can provide some guide to control the contribution of elastic instabilities to the sliding friction force which is of important practical significance.

During part of this work, A.N. was supported by the "Graduiertenförderung der Universität Leipzig". A.B. and A.P. acknowledge the support of the Chemistry Division of the Office of Naval Research Laboratory. We want to acknowledge the hospitality of the Experimentalphysik V department of the University of Bayreuth where part of the experiments have been performed. We thank H. Brandt, P. Allen and S. Hunklinger for discussions and A. Setzer for technical assistance. This work is supported by the Deutsche Forschungsgemeinschaft under DFG Es 86/4-2.

## References

1. P.W. Anderson, B.I. Halperin, C.M. Varma, Phil. Mag. **25**, 1 (1972); W.A. Phillips, J. Low Temp. Phys. **7**, 351 (1972).
2. See for example the data compilation presented by J. Berret, M. Meißner, Z. Phys. B **70**, 65 (1989).
3. A. Burin, Yu. Kagan, Sov. Phys. JETP **109**, 299 (1996); for a recent review covering the effect of interaction see: A.L. Burin, D. Natelson, D.D. Osheroff, Yu. Kagan in *Tunneling*

*Systems in Amorphous and Crystalline Solids*, edited by P. Esquinazi (Springer Verlag, Heidelberg, Berlin, New York, Tokio, 1998), Chap. 5.
4. E. Gaganidze, R. König, P. Esquinazi, K. Zimmer, A. Burin, Phys. Rev. Lett. **79**, 5038 (1997).
5. M.W. Klein *et al.*, Phys. Rev. B **18**, 5887 (1987).
6. C.C. Yu, A.J. Leggett, Comm. Cond. Matter Phys. **14**, 231 (1989).
7. J.J. Freeman, A.C. Anderson, Phys. Rev. B **34**, 5684 (1986).
8. ALFA, No. 36669 and No. 12727.
9. Goodfellow, Teflon powder 6–9 $\mu$m, No. FP306010.
10. ALFA, No. 88316.
11. The grain size has been measured with a Laser Particle Size Analysette from Fritsch.
12. Vycor Glass 7930, Corning Glass Works, Houghton Park, Corning, NY 14831, USA.
13. P. Levitz, G. Ehret, S. Sinha, J. Drake, J. Chem. Phys. **95**, 6151 (1991).
14. M. Deye, P. Esquinazi, Z. Phys. B **76**, 283 (1989).
15. A. Nittke, M. Scherl, P. Esquinazi, W. Lorenz, Li Junyun, F. Pobell, J. Low Temp. Phys. **98**, 517 (1995).
16. For a recent review on heat release in solids see: A. Nittke, S. Sahling, P. Esquinazi in *Tunneling Systems in Amorphous and Crystalline Solids*, edited by P. Esquinazi (Springer Verlag, Heidelberg, Berlin, New York, Tokyo, 1998), Chap. 2.
17. J.L. Black, Phys. Rev. B **17**, 2740 (1978).
18. D.A. Parshin, S. Sahling, Phys. Rev. B **47**, 5677 (1993).
19. B. Neppert, P. Esquinazi, Cryogenics **36**, 231 (1996).
20. M. Schwark, F. Pobell, M. Kubota, R.M. Mueller, J. Low Temp. Phys. **58**, 171 (1985).
21. J.C. Lasjaunias, A. Ravex, M. Vandorpe, S. Hunklinger, Solid State Commun. **17**, 1045 (1975).
22. A.M. de Goer, R. Calemczuk, B. Salce, J. Bon, E. Bonjour, R. Maynard, Phys. Rev. B **40**, 8327 (1989).
23. T. Sleator, A. Bernasconi, E. Felder, D. Posselt, H. Ott, Physica B **165–166**, 907 (1990).
24. A. Efros, Shklovskii, in *Electron-Electron Interaction in Disordered Systems*, edited by A.L. Efros, M. Pollak (North Holland, Amsterdam, 1985).
25. A. Burin, Yu. Kagan, Physica B **91**, 367 (1993).
26. S. Hunklinger, A.K. Raychaudhuri, Progr. Low Temp. Phys. **9**, 267 (1986).
27. X. Liu, B.E. White Jr., R.O. Pohl, E. Iwanizcko, K.M. Jones, A.H. Mahan, B.N. Nelson, R.S. Grandall, S. Verpek, Phys. Rev. Lett. **78**, 4418 (1997).
28. B.E. White, Jr., R.O. Pohl, Phys. Rev. Lett. **75**, 4437 (1995).
29. M. von Haumeder, U. Strom, S. Hunklinger, Phys. Rev. Lett. **44**, 84 (1980).
30. For a recent review on this issue see M. Ramos, U. Buchenau, in *Tunneling Systems in Amorphous and Crystalline Solids*, edited by P. Esquinazi (Springer Verlag, Heidelberg, Berlin, New York, Tokio, 1998), Chap. 9.
31. T. Baumberger, Solid State Commun. **102**, 175 (1997).